Accepted Manuscript

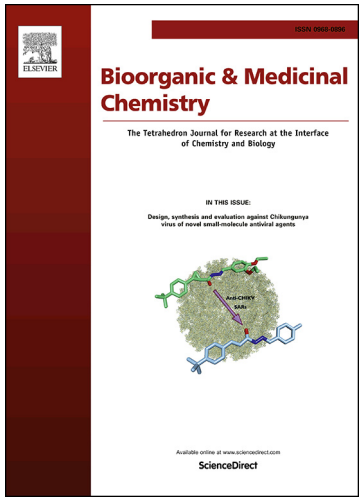

Novel 4-aminoquinazoline derivatives induce growth inhibition, cell cycle arrest and apoptosis via PI3Kα inhibition

Yan-Hua Fan, Huai-Wei Ding, Dan-Dan Liu, Hong-Rui Song, Yong-Nan Xu, Jian Wang

PII: S0968-0896(17)32441-0
DOI: https://doi.org/10.1016/j.bmc.2018.02.015
Reference: BMC 14201

To appear in: *Bioorganic & Medicinal Chemistry*

Received Date: 19 December 2017
Revised Date: 3 February 2018
Accepted Date: 12 February 2018

Please cite this article as: Fan, Y-H., Ding, H-W., Liu, D-D., Song, H-R., Xu, Y-N., Wang, J., Novel 4-aminoquinazoline derivatives induce growth inhibition, cell cycle arrest and apoptosis via PI3Kα inhibition, *Bioorganic & Medicinal Chemistry* (2018), doi: https://doi.org/10.1016/j.bmc.2018.02.015

This is a PDF file of an unedited manuscript that has been accepted for publication. As a service to our customers we are providing this early version of the manuscript. The manuscript will undergo copyediting, typesetting, and review of the resulting proof before it is published in its final form. Please note that during the production process errors may be discovered which could affect the content, and all legal disclaimers that apply to the journal pertain.

ACCEPTED MANUSCRIPT

Novel 4-aminoquinazoline derivatives induce growth inhibition, cell cycle arrest and apoptosis via PI3Kα inhibition

Yan-Hua Fan [b], Huai-Wei Ding [a,*], Dan-Dan Liu [a], Hong-Rui Song [a], Yong-Nan Xu [a], Jian Wang [a]

[a] Key Laboratory of Structure-Based Drug Design and Discovery, Ministry of Education, Shenyang Pharmaceutical University, Shenyang 110016, China

[b] Wuya College of Innovation, Shenyang Pharmaceutical University, Shenyang 110016, China

* Corresponding authors.

Email address: dinghuaiwei627@163.com.

ACCEPTED MANUSCRIPT

ACCEPTED MANUSCRIPT

Abstract: Phosphatidylinositol 3-kinase (PI3K) signaling pathway has diverse functions, including the regulation of cellular survival, proliferation, cell cycle, migration, angiogenesis and apoptosis. Among class I PI3Ks (PI3Kα, β, γ, δ), the PIK3CA gene encoding PI3K p110α is frequently mutated and overexpressed in a large portion of human cancers. Therefore, the inhibition of PI3Kα has been considered as a promising target for the development of a therapeutic treatment of cancer. In this study, we designed and synthesized a series of 4-aminoquinazoline derivatives and evaluated their antiproliferative activities against six cancer cell lines, including HCT-116, SK-HEP-1, MDA-MB-231, SNU638, A549 and MCF-7. Compound **6b** with the most potent antiproliferative activity and without obvious cytotoxicity to human normal cells was selected for further biological evaluation. PI3K kinase assay showed that **6b** has selectivity for PI3Kα distinguished from other isoforms. The western blot assay and PI3K kinase assay indicated that **6b** effectively inhibited cell proliferation via suppression of PI3Kα kinase activity with an IC_{50} of 13.6 nM and subsequently blocked PI3K/Akt pathway activation in HCT116 cells. In addition, **6b** caused G1 cell cycle arrest owing to the inhibition of PI3K signaling and induced apoptosis via mitochondrial dependent apoptotic pathway. Our findings suggested that **6b** has a therapeutic value as an anticancer agent via PI3Kα inhibition.

Keywords: PI3K inhibitor; 4-aminoquinazoline; antiproliferative effects; cell cycle arrest; apoptosis

ACCEPTED MANUSCRIPT

ACCEPTED MANUSCRIPT

1. Introduction

The phosphatidylinositol 3-kinases (PI3K) families are divided into four different classes: Class I, Class II, Class III and Class IV. The most studied are the class I enzymes which are further divided into PI3Kα, PI3Kβ, PI3Kδ and PI3Kγ [1-2]. PI3K pathway regulates various cellular processes, such as proliferation, growth, cell cycle, autophagy and apoptosis [3-6]. Hyperactivation of the PI3K/Akt pathway has been confirmed as an essential step in the initiation and maintenance of human tumors [5-8]. An accumulation of evidence indicates that PI3K pathway plays a key role in the regulation of cell cycle and apoptosis [9-10]. The PI3K pathway becomes activated during the G1/S transition of the cell cycle and regulates several key cell cycle regulators, including $p21^{Cip1}$, CyclinD, and $p27^{Kip1}$ protein stability [10]. It is known that hyperactive PI3K/Akt signaling prevents apoptosis. PI3K increases Mdm2 protein levels and causes a reduction of p53 [11-12]. Bcl-2 family plays an instrumental role in the regulation of apoptosis [13]. PI3K/Akt pathway mediates cell viability and apoptosis via Bcl-2 family proteins including Bad and Bcl-2, which is a crucial regulator of the mitochondrial apoptosis pathway [14]. Therefore, PI3K inhibition will cause cell apoptosis via p53 and mitochondrial apoptosis pathway.

Given the important role of PI3K played in the occurrence and development of human tumors [15-18], a lot of PI3K inhibitors have been developed and are being evaluated in preclinical studies and early clinical trials [19-21]. Among them, BEZ235 has been identified as highly potent inhibitor of PI3K and is currently under evaluation in clinical trials for oncology applications [22]. The other two BEZ235 analogues BGT226 [23] and PF-04979064 [24] were also being evaluated in preclinical studies and early clinical trials. In addition, GSK2126458 and HS-173 which all have sulfonamide pyridyl both exhibited potent and highly selective PI3Kα inhibitory activity with an IC_{50} of picomolar level

ACCEPTED MANUSCRIPT

[25-27].

Quinazoline derivatives, especially 4-anilinoquinazolines, have attracted interests over the years for their multiple biological activities, notably as EGFR inhibitors [28]. Numerous drugs containing quinazoline moiety have been successfully developed, such as Gefitinib, Lapatinib, Erlotinib, Vandetanib and Afatinib. Thereby, we designed and synthesized a new series of 4-aminoquinazoline derivatives containing 6-sulfonamide substituted pyridyl group. In addition, we evaluated the anti-tumor effects of all these prepared compounds and investigated their anti-tumor pharmacologic mechanism *in vitro*.

2. Results and discussion

2.1 Chemistry

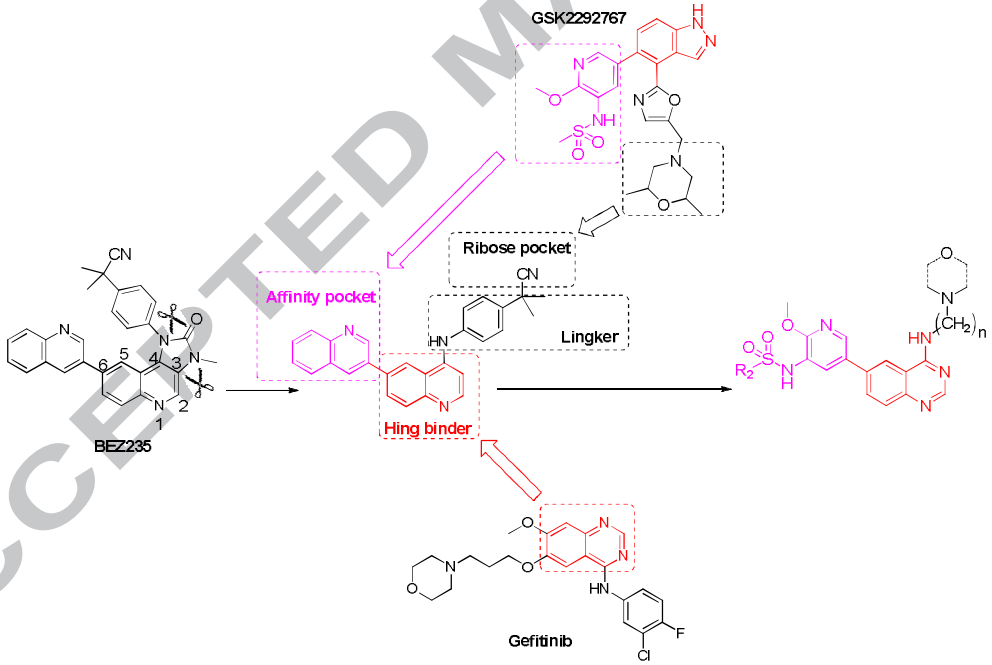

Fig.1. The design strategy based on NVP-BEZ235 and GSK2292767.

We had a good understanding of the binding mode of PI3K inhibitors based on the analysis of the reported crystal structure complexes and reviews [19, 25, 27]. Most of the PI3K inhibitors have very similar binding modes and the active sites of PI3K kinase are mainly composed of three regions: the

ACCEPTED MANUSCRIPT

hinge binder domain, the affinity pocket domain and the ribose pocket domain (Fig.1).

Quinazoline is an important scaffold in drug discovery and 4-aminoquinazoline derivatives had been reported as PI3K inhibitors in recent years [29-32]. So, we believe that the quinazoline group still has good prospects for development. In order to develop new PI3K inhibitors containing quinazoline structure, we opened the five ring of BEZ235 and the quinazoline ring was used instead of the quinoline ring. Next, we introduce hydrophilic groups on the position-4 of quinazoline nucleus and the "affinity pocket" was filled by sulfonamide pyridine instead of the quinoline ring.

2.2 Antiproliferative assays in vitro

All synthesized compounds were evaluated for their cytotoxicity *in vitro* against six human cancer cell lines including HCT116, A549, SK-HEP-1, SNU638, MDA-MB-231 and MCF-7 cells. The antiproliferative results of all the compounds were summarized in Table 1. The results of antiproliferative effect assay showed most of the derivatives exhibited potent antiproliferative effects, especially against HCT-116. Notably, **6b** showed the most significant antiproliferative activity against all these cancer cell lines. From compounds **6a-6d** (IC_{50} = 13.5, 0.16, 3.20 and 1.44 μM against HCT-116 separately), which all have a common 4-*N, N*-dimethylethane-1,2-diamine-quinazoline moiety with different sulfonamide groups. Compared to 4-fluorophenyl, 2,4-difluorophenyl at R_2 position markedly improved antiproliferative activity and N-butyl at R_2 position showed the best antiproliferative activities. The structure-activity relationships (SARs) indicated that butyl sulfonamide and 2,4-difluorosulfonamide were beneficial to the enhancement of anti-tumor activity, so the subsequent synthesis retained both sulfonamides and only changed the ammonia on the position-4 of quinazoline. Compound **6b** and **6e** (IC_{50} = 0.49 μM against HCT-116), **6d** and **6f** (IC_{50} = 2.20 μM against HCT-116), **6g** (IC_{50} = 0.59 μM against HCT-116) and **6i** (IC_{50} =

ACCEPTED MANUSCRIPT

1.74 μM against HCT-116), **6h** (IC_{50} = 2.74 μM against HCT-116) and **6j** (IC_{50} = 18.8 μM against HCT-116), suggesting that two carbon atoms in the R_1 group was better than that of the three carbon atoms. Compound **6a** - **6j** more potent than **6k** (IC_{50} = 5.72 μM against HCT-116) and **6l** (IC_{50} = 17.6 μM against HCT-116), indicating that alkyl group at position of R_1 is more beneficial to activity than aromatic group.

Table 1 Cytotoxicity *in vitro* of target compounds against five cancer cell lines (IC_{50} Values[a] in μM).

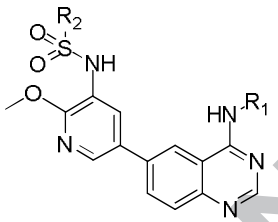

Comp.	R_1	R_2	IC_{50} (μM)					
			HCT-116	SK-HEP1	MDA-MB -231	SNU638	A549	MCF-7
6a	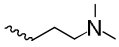		13.5±0.27	12.6±0.22	2.32±0.07	0.41±0.02	4.12±0.15	14.7±0.34
6b	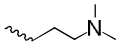		0.16±0.01	0.28±0.02	0.28±0.03	0.48±0.04	1.32±0.05	3.24±0.08
6c	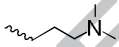	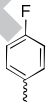	3.20±0.06	9.50±0.14	1.22±0.04	1.21±0.05	2.42±0.08	1.23±0.04
6d			1.44±0.06	4.72±0.09	0.71±0.04	0.62±0.03	0.94±0.06	1.02±0.07
6e	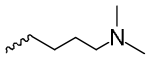		0.49±0.05	0.86±0.06	0.88±0.07	1.26±0.08	3.52±0.12	4.73±0.14
6f	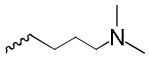		2.20±0.04	4.68±0.07	1.54±0.03	1.26±0.02	2.78±0.06	3.66±0.07

ACCEPTED MANUSCRIPT

6g	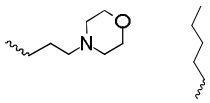	0.59±0.01	0.44±0.01	0.42±0.02	0.61±0.03	1.56±0.04	10.8±0.16
6h	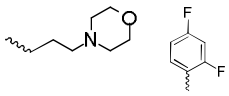	2.74±0.06	0.84±0.06	0.38±0.04	3.96±0.09	0.62±0.08	28.9±0.24
6i	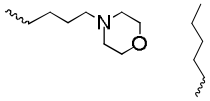	1.74±0.04	1.14±0.03	2.58±0.07	0.98±0.03	3.14±0.08	4.59±0.07
6j	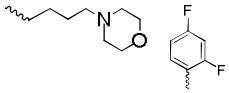	18.8±0.26	13.4±0.15	8.96±0.10	4.52±0.08	9.82±0.12	13.5±0.14
6k	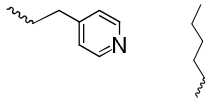	5.72±0.08	8.98±0.11	4.32±0.08	6.66±0.12	9.42±0.14	18.7±0.22
6l	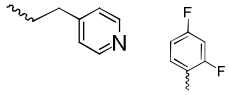	17.6±0.18	12.4±0.14	9.71±0.09	6.21±0.04	11.4±0.08	22.5±0.34
BEZ235		0.84±0.12	1.82±0.23	0.18±0.02	1.24±0.13	0.62±0.07	1.33±0.14

[a]IC_{50} values are the mean of triplicate measurements.

We also test the cytotoxic effects of **6b** on normal human cells MRC5 and HEK293. We obserbed **6b** showed much less inhibitory activity against human normal cells (IC_{50} = 18.5 μM against MRC5 and IC_{50} = 12.6 μM against HEK293), implying the possibility of inhibition of cancer cells without any effects on normal cells (Table 2).

Table 2 Cytotoxicity of **6b** to normal human cells (IC_{50} Values in μM)

Cells	MRC5	HEK293
6b	18.5	12.6

*2.3 **6b** inhibits PI3Kα and blocks the PI3K-Akt pathway in HCT116 cells*

6b was found to inhibit PI3Kα with an IC_{50} of 13.6 nM (Table 3). Docking simulations were

ACCEPTED MANUSCRIPT

conducted to predict the binding mode of **6b** and PI3Kα using Autodock 4.2 (Fig. 2). On the basis of the docking model results, there is a hydrogen bond formed between the nitrogen atom of *N*, *N*-dimethylethanamine group and the NH group of the catalytic lysine (Lys802). Moreover, the sulfonamide formed two additional hydrogen interactions with Gln859 and Thr856. In addition to these, the nitrogen atoms of quinazolin moiety form two key hydrogen bond with the conserved water molecule. These multiple hydrogen bonds and some other interaction including van der Waals forces, aromatic stacking interaction, electrostatic interaction and hydrophobic interaction appeared to be the most significant binding force stabilizing **6b** in the active site of PI3Ka. To analyze the binding affinity of 6b and other PI3K isoforms, we also conducted docking simulations to predict their binding mode. As shown in Fig. S1, unlike PI3Kα, no such interactions between the Alkyl sidechain at the 4-quinoline position and **6b** were formed in the active site of other three PI3K isoforms, indicating this Alky sidechain played a key role on enhancement of PI3Ka inhibitory potency of 6b and may offer a selective inhibition to PI3Kα.

Table 3 Activities of **6b** and **BEZ235** against Class I PI3K (IC_{50} Values in nM)

	PI3Kα	PI3Kβ	PI3Kγ	PI3Kδ
6b	13.6	396.2	117.5	101.8
BEZ235	16.4	35.9	23.6	78.4

ACCEPTED MANUSCRIPT

ACCEPTED MANUSCRIPT

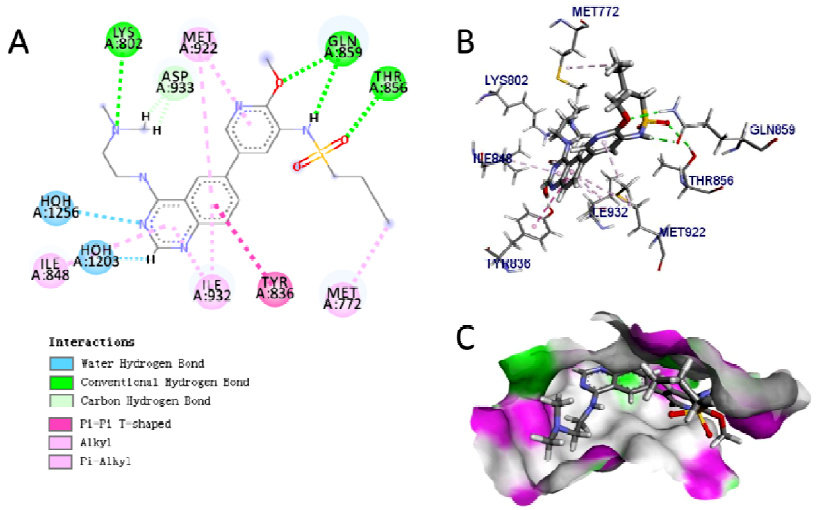

Fig.2. The binding model of **6b** bound to PI3Kα. Autodock 4.2 programs were used to perform this molecular docking simulation. (A) 2D binding model of **6b** and PI3Kα. (B-C) 3D binding model of **6b** and PI3Kα.

Because **6b** suppressed PI3Kα activity, we concluded that downstream of PI3K signaling that mediates cell growth and blocks cell apoptosis might also be inhibited by **6b**. Therefore, we assessed whether **6b** changed the expression of the PI3K/Akt signaling pathways and their downstream signaling molecules by western blot analysis. Compared to the control group, the levels of p-PI3K, p-Akt (Ser473) and p-GSK3β were significantly decreased by **6b** in HCT116 cells. In addition, the suppressive effect of **6b** on p-Akt expression was also confirmed by immunofluorescence analysis under a confocal microscope after treatment of **6b** for 8 h.

ACCEPTED MANUSCRIPT

ACCEPTED MANUSCRIPT

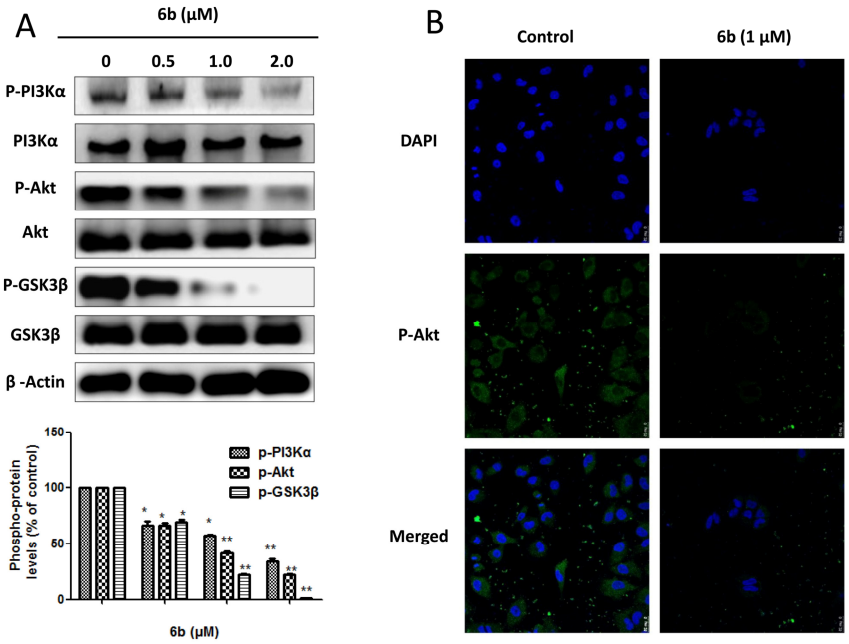

Fig.3. 6b suppresses PI3K signaling pathway. (A) The effects of **6b** on the expressions of PI3K-associated signaling proteins in HCT116 cells. (B) The effects of **6b** on the expression level of p-Akt (Ser473) in cells as determined by immunofluorescence analysis. Cells were treated with the indicated concentrations of **6b** for 24 h and then the protein expressions were determined by using Western blot. The alternations of related proteins were quantified using Image J program. **P*<0.05 or ***P*<0.01 was considered statistically significant compared with corresponding control values.

*2.4 **6b** induce G1 phase arrest in HCT116 and NCI-H1975 cells*

To better elucidate the antitumor mechanism responsible for antiproliferation and induction of apoptosis of **6b**, the cell cycle distribution was evaluated by flow cytometric analysis. As shown in the cell cycle data showed that **6b** induced an obvious accumulation of cells in G1 phase and reduced the percentage of cells at the S phase compared with the control group in HCT116 cells. These results are consistent with cell cycle arrest due to the inhibition of PI3K kinase activity.

ACCEPTED MANUSCRIPT

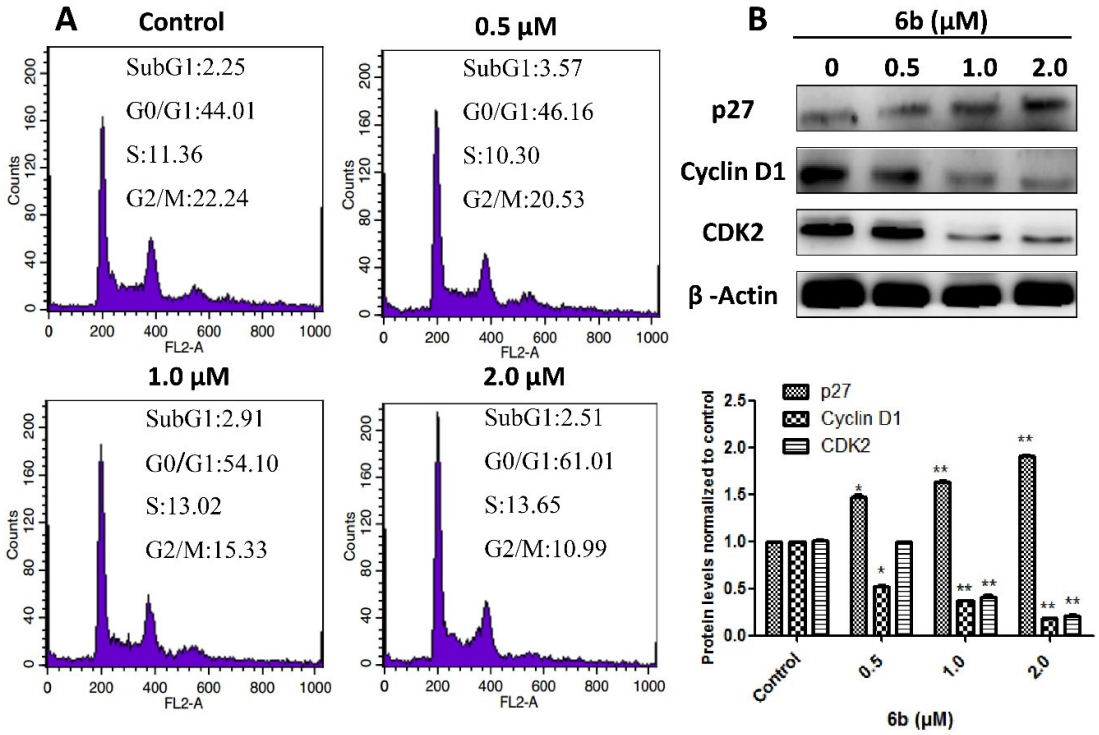

Fig.4. 6b induced G1 cell cycle arrest in HCT116 cells. (A) Cells were treated with the indicated concentrations of **6b** for 24 h. The DNA content of the cells was then analyzed by flow cytometry analysis as described in Materials and Methods. (B) Cells were treated with the indicated concentrations of **6b** for 24 h and then analyzed the protein expressions associated with the G1 phase cell cycle arrest in HCT116 cells. The changes of corresponding proteins were quantified using Image J. Each bar represents mean ± SEM (n = 3), *P<0.05 or **P<0.01 was considered statistically significant compared with corresponding control values.

*2.5 **6b** induced cell apoptosis via the mitochondrial pathway*

Since PI3K/Akt pathway is well known as a pro-survival mechanism in many cancer cells, we want to know whether **6b** induced apoptosis in HCT116 cells. Flow cytometric analysis data showed the percentage of Annexin V-positive cells was significantly increased after exposure to increasing dose of **6b**, compared with medium control (5.15% vs 15.71% for HCT116, P < 0.01). These results

ACCEPTED MANUSCRIPT

suggested that compound **6b** can induce apoptosis *in vitro* and this is one of mechanisms by which compound **6b** exerted its antiproliferative activity.

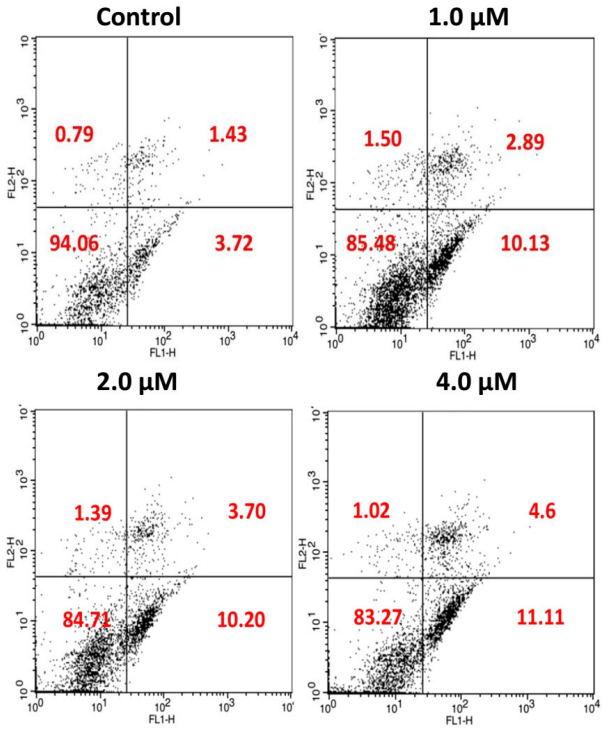

Fig.5. 6b induced apoptosis in HCT116 cells. Cells were treated with various concentrations of **6b** for 48 h and then analyzed the Annexin V-FITC/PI staining test by flow cytometry analysis. The number in the right quads of each panel means the percentage of Annexin V positive cells.

To confirm the effects of **6b** on apoptosis induction, we examined the changes in apoptotic related proteins in HCT116 after treatment with **6b** for 48 h. In comparison to the control, the cleaved caspase-9 and cleaved caspase-3 levels were remarkably boosted when treated with **6b** at 4 μM. In addition, the level of cleaved PARP was also elevated by **6b** treatment for 48 h in HCT116 cells. Taken together, these results indicated that **6b** induced apoptosis in HCT116 cells via the mitochondrial pathway.

ACCEPTED MANUSCRIPT

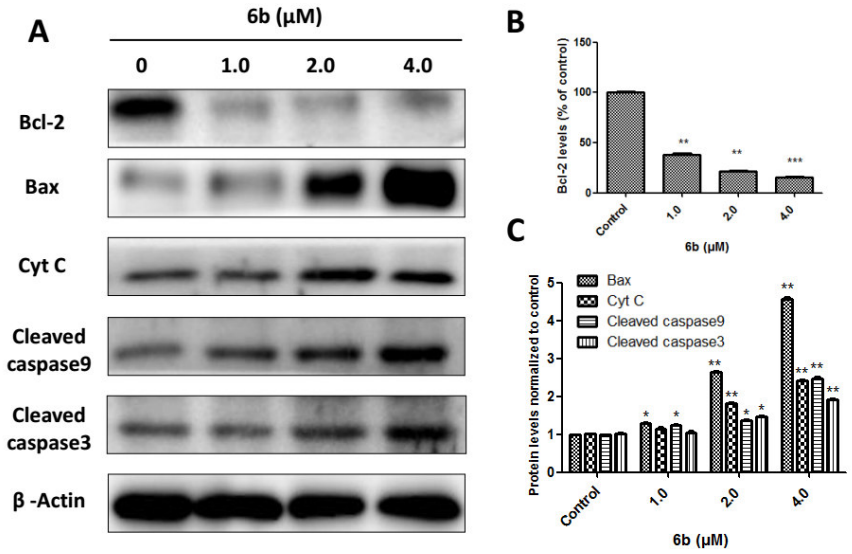

Fig.6. (**A**) The effects of **6b** on the induction of apoptosis were also analyzed by Western blot in HCT116. The changes of corresponding proteins were quantified using Image J. Each bars represent mean ± SE (n = 3). **P*<0.05 or ***P*<0.01 was considered statistically significant compared with corresponding control values.

3. Discussion and conclusion

PI3K/Akt signaling pathway is continuously active in many cancers promoting cell viability and results in resistance to chemotherapy [33]. Numerous studies have indicated that somatic mutations in genes associate with PI3K/Akt/mTOR pathway increase Akt activity and show an antagonism to chemotherapy and radiation induced apoptosis [34]. High frequency of somatic mutations in PIK3CA has been reported in many kinds of human cancer, suggesting that mutated PIK3CA gene as an oncogene in cancers [35]. Therefore, PI3Kα has been extensively studied and explored as a target for the development of cancer drug. In theory, PI3Kα-selective inhibitors should provide more specific inhibition of PI3Kα while reducing the side effects caused by non-selective blockade of other PI3K isoforms. Recently, lots of PI3Kα inhibitors were designed and synthesized from all kinds of structural scaffolds including quinazoline derivatives.

An increasing number of studies showed that quinazoline derivatives are of considerable

ACCEPTED MANUSCRIPT

pharmacological chemicals as anticancer agents [36]. Quinazoline moiety has been extensively used as a drug-like scaffold in medicinal chemistry, especially in the development of anticancer agents [37]. Several quinazoline derivatives are potent and highly selective inhibitors of tyrosine kinase, such as gefitinib, erlotinib, lapatinib, and afatinib, have been successfully developed and used in clinical trials in the past few years[17-19]. Therefore, in recent years, the synthesis of 4-aminoquinazolines has attracted much attention.

In this study, we designed and synthesized a serial of 4-aminoquinazoline derivatives based on NVP-BEZ235 and GSK2292767. The *in vitro* antiproliferative activities of all the prepared chemicals were evaluated against six human cancer cell lines and two normal human cells. Although a potential growth inhibitory activity of **6b** was found in cultured human lung cancer cell lines, **6b** did not exhibit a considerable anti-proliferative activity against MRC-5 human lung normal epithelial cells (IC_{50} of 18.5 μM) and HEK293 human embryonic kidney cells (IC_{50} of 12.6 μM) indicating that **6b** selectively inhibits the proliferation of cancer cells compared to normal cells (Table 2). Among of these compounds, compound **6b** effectively inhibited the PI3K kinase activity, in particularly PI3Kα (Table 3) and markedly induced a dose dependent suppression of the phosphorylation of Akt and its downstream factor GSK3β (Fig.3). In addition, **6b** also induced G1 phase cell cycle arrest through regulation of G1 phase related targets, which is consistent with the effects of some PI3K inhibitors (Fig.4). We next determined if **6b** caused apoptosis in HCT116 cells. Annexin V-PI staining showed **6b** enhanced the cell apoptosis after treatment for 48 h (Fig.5). Western blot analysis indicated that **6b** strongly reduced Bcl-2 levels and increased the Bax levels. In addition, **6b** induced cell apoptosis in HCT116 cells via increasing cytochrome C and the activated caspase 3 and caspase 9 (Fig.6).

In summary, we designed and synthesized a series of compounds containing hydrophilic group

ACCEPTED MANUSCRIPT

in position-4 of quinazoline and evaluated their antiproliferative activities against six cancer cell lines, including HCT-116, A549, SK-HEP-1, SNU638, MDA-MB-231 and MCF-7. Compound **6b**, with the most potent antiproliferative activity was selected for further biological evaluation. Our further study showed that the suppression of cell survives and growths induced by **6b** via PI3K/Akt/mTOR pathway inhibition. In addition, inhibition of PI3K signaling by **6b** further resulted in G1 cell cycle arrest and cell apoptosis. These findings suggest that **6b** may be used as a potential PI3K inhibitor to treat human cancers.

4. Material and methods

4.1 Chemistry

4.1.1 Instruments & chemicals

All reagents and solvents were commercially available without further purification. ^{1}H NMR spectra and ^{13}C NMR spectra were recorded on 400 and 600 Bruker NMR spectrometer with tetramethylsilane (TMS) as an internal standard. All chemical shifts are reported in ppm (δ) and coupling constants (J) are in hertz (Hz). All the melting points were determined on a Beijing micromelting-point apparatus and thermometer was uncorrected. High-resolution exact mass measurements were performed using electrospray ionization (positive mode) on a quadrupole time-of-flight (QTOF) mass spectrometer (microTOF-Q, Bruker Inc.).

4.1.2 General experimental protocol for preparation of compounds

The synthetic routes for the target compounds are outlined in Schemes 1. Sulfonylation of **1** with four benzenesulfonyl chlorides to yield **2a**-**d**, which were then subjected to Suzuki coupling with bis(pinacolato)diborane to afford arylboronic ester **3a**-**d**. Intermediate **4** was reacted with five amines

ACCEPTED MANUSCRIPT

to abtain **5a-e**, which were coupled with **3a-d** via Suzuki reaction to afford the target compounds **6a-l**.

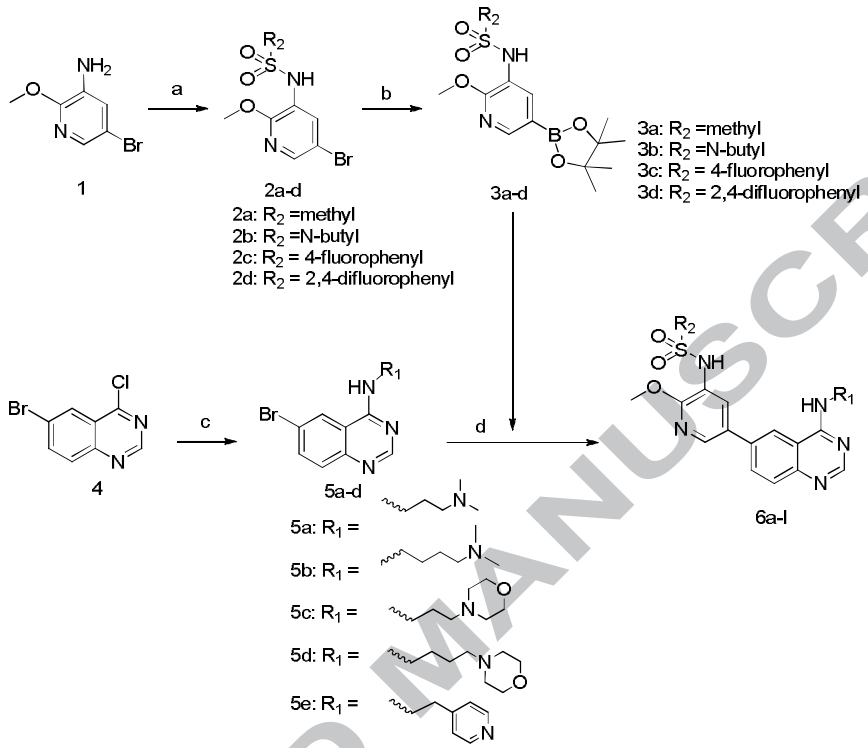

Scheme 1. (a) benzenesulfonyl chloride, pyridine, rt, 24 h; (b) bis(pinacolato)diborane, $Pd(dppf)_2Cl_2$, AcOK, DMF, 100 ºC, 8 h; (c) amines, isopropanol, 50 ºC, 1h; (d) $Pd(dppf)_2Cl_2$, Cs_2CO_3, DMF/ H_2O, 90 ºC, 8 h.

*4.1.2.1 N-(5-bromo-2-methoxypyridin-3-yl)methanesulfonamide (**2a**)*

To a solution of 5-bromo-2-methoxypyridin-3-amine (**1**) (2.01 g, 10 mmol) in pyridine (50 ml) at 0 ºC was added methanesulfonyl chloride (1.25 g, 11 mmol). Then the mixture was stirred at room temperature for 24 h. Pyridine was removed under reduced pressure before adding water (100 ml), then extracted with ethyl acetate (3 × 100 ml), the organic layer was washed with water (50 ml), dried with Na_2SO_4 and evaporated to give compound **2a** as a white solid (2.42 g, 86.5%). mp 136-138 ºC.^{1}H NMR(400 MHz, DMSO-d_6) δ 9.49 (s, 1H, NH), 8.09 (d, J = 2.4 Hz, 1H, Ar-H), 7.79 (d, J = 2.0 Hz, 1H, Ar-H), 3.91(s, 3H, OCH_3), 3.11(s, 3H, CH_3). ESI-MS: m/z 280.1 $[M+H]^+$.

ACCEPTED MANUSCRIPT

Compounds **2b**-**d** were synthesized according to the procedure described in **2a**.

*4.1.2.2 N-(5-bromo-2-methoxypyridin-3-yl)butane-1-sulfonamide (**2b**)*

78.4% yield. mp 150-151 ºC.9.51 (s, 1H, NH), 8.09 (d, *J* = 2.4 Hz, 1H, Ar-H), 7.77 (d, *J* = 2.4Hz, 1H, Ar-H), 3.91 (s, 3H, OCH_3), 3.16 (t, *J* = 7.6Hz, 2H, CH_2), 1.73 - 1.65 (m, 2H, CH_2), 1.42 - 1.33 (m, 2H, CH_2), 0.87 (t, *J* = 7.2 Hz, 3H, CH_3). ESI-MS: m/z 323.1 $[M+H]^+$.

*4.1.2.3 N-(5-bromo-2-methoxypyridin-3-yl)-4-fluorobenzenesulfonamide (**2c**)*

89.4% yield. mp 152-154 ºC.^{1}H NMR (400 MHz, DMSO) δ 10.22 (s, 1H, NH), 8.08 (d, *J* = 2.2 Hz, 1H, Ar-H), 7.83 (dd, *J* = 8.8, 5.2 Hz, 2H, Ar-H), 7.72 (d, *J* = 2.2 Hz, 1H, Ar-H), 7.43 (t, *J* = 8.8 Hz, 2H, Ar-H), 3.64 (s, 3H, OCH_3). ESI-MS: m/z 385.1 $[M+H+Na]^+$.

*4.1.2.4 N-(5-bromo-2-methoxypyridin-3-yl)-2,4-difluorobenzenesulfonamide (**2d**)*

85.6% yield. mp 163-165 ºC. ^{1}H NMR (400 MHz, DMSO) δ 10.46 (s, 1H, NH), 8.13 (d, *J* = 2.2 Hz, 1H, Ar-H), 7.83-7.74 (m, 2H, Ar-H), 7.62-7.52 (m, 1H, Ar-H), 7.24 (td, *J* = 2.0, 8.5 Hz, 1H, Ar-H), 3.62 (s, 3H, OCH_3). ESI-MS: m/z 376.9 $[M-H]^+$.

4.1.2.5

*N-(2-methoxy-5-(4,4,5,5-tetramethyl-1,3,2-dioxaborolan-2-yl)pyridin-3-yl)methanesulfonamide (**3a**)*

A solution of the **2a** (2.80 g, 10 mmol), bis(pinacolato)diborane (1.27 g, 5 mmol), $Pd(dppf)_2Cl_2$ (0.18 g, 0.25 mmol) and KOAc (1.47 g, 15 mmol) in anhydrous DMF (30 ml) under N_2 was stirred at 100 ºC for 8 h. DMF was removed under reduced pressure and adding water (100 ml), extracted with ethyl acetate (3 × 100 ml), the organic layer was washed with water (20 ml), dried with Na_2SO_4 and evaporated to give compound **3a** as a white solid (1.98 g, 60.4% yield). mp 90-92 ºC. ^{1}H NMR (400 MHz, DMSO) δ 9.25 (s, 1H, NH), 8.21 (d, *J* = 1.6 Hz, 1H, Ar-H), 7.78 (d, *J* = 1.6 Hz, 1H, Ar-H), 3.94 (s, 3H, OCH_3), 3.01 (s, 3H, CH_3), 1.30 (s, 12H, CH_3). ESI-MS: m/z 329.1 $[M+H]^+$.

ACCEPTED MANUSCRIPT

Compounds **3b**-**d** were synthesized according to the procedure described in **3a**.

4.1.2.6

*N-(2-methoxy-5-(4,4,5,5-tetramethyl-1,3,2-dioxaborolan-2-yl)pyridin-3-yl)butane-1-sulfonamide (**3b**)*

64.3% yield. mp 91-92 ºC.^{1}H NMR (400 MHz, DMSO) δ 9.26 (s, 1H, NH), 8.21 (d, *J* = 1.4 Hz, 1H, Ar-H), 7.79 (d, *J* = 1.3 Hz, 1H, Ar-H), 3.94 (s, 3H, OCH_3), 3.10 - 3.01 (m, 2H, CH_2), 1.76 - 1.63 (m, 2H, CH_2), 1.38 (dt, *J* = 7.4, 14.8Hz, 2H, CH_2), 1.30 (s, 12H, CH_3), 0.86 (t, *J* = 7.3 Hz, 3H, CH_3). ESI-MS: m/z 371.2 $[M+H]^+$.

4.1.2.7

*4-fluoro-N-(2-methoxy-5-(4,4,5,5-tetramethyl-1,3,2-dioxaborolan-2-yl)pyridin-3-yl)benzenesulfonamide (**3c**)*

74.5% yield. mp 149-151 ºC. ^{1}H NMR (400 MHz, DMSO) δ 9.92 (s, 1H, NH), 8.18 (s, 1H, Ar-H), 7.73 (m, 3H, Ar-H), 7.40 (t, *J* = 8.7 Hz, 2H, Ar-H), 3.62 (s, 3H, OCH_3), 1.29 (s, 12H, CH_3). ESI-MS: m/z 409.3 $[M+H]^+$.

4.1.2.8

*2,4-difluoro-N-(2-methoxy-5-(4,4,5,5-tetramethyl-1,3,2-dioxaborolan-2-yl)pyridin-3-yl)benzenesulfonamide (**3d**)*

78.8% yield. mp 171-173 ºC. ^{1}H NMR (400 MHz, DMSO) δ 10.19 (s, 1H, NH), 8.21 (d, *J* = 1.5 Hz, 1H, Ar-H), 7.72 (d, *J* = 1.5 Hz, 1H, Ar-H), 7.71 - 7.67 (m, 1H, Ar-H), 7.59 - 7.54 (m, 1H, Ar-H), 7.20 (td, *J* = 2.0, 8.6 Hz, 1H, Ar-H), 3.62 (s, 3H, OCH_3), 1.30 (s, 12H, CH_3). ESI-MS: m/z 427.3 $[M+H]^+$.

*4.1.2.9 N-(6-bromoquinazolin-4-yl)-N,N-dimethylethane-1,2-diamine (**5a**)*

ACCEPTED MANUSCRIPT

A solution of the **4** (0.24 g, 1 mmol), *N*,*N*-dimethylethane-1,2-diamine (0.13g, 1.5 mmol) in isopropanol (20 ml) were stirred at 50 ºC for 1 h. Isopropanol was removed under reduced pressure and the residue was purified through a column chromatography on silica with chloroform/methanol (V:V 20:1) as a white solid (0.27 g, 92.0% yield). mp 132-134 ºC. ^{1}H NMR (600 MHz, DMSO) δ 8.56 (d, *J* = 2.1 Hz, 1H, Ar-H), 8.48 (s, 1H, Ar-H), 8.34 (t, *J* = 5.3 Hz, 1H, NH), 7.88 (dd, *J* = 8.8, 2.2 Hz, 1H, Ar-H), 7.62 (d, *J* = 8.8 Hz, 1H, Ar-H), 3.63 (dd, *J* = 12.3, 6.6 Hz, 2H, CH_2), 2.52 (t, *J* = 6.6 Hz, 2H, CH_2), 2.20 (s, 6H, CH_3). ESI-MS: m/z 295.2 $[M+H]^+$.

Compounds **5b-e** were synthesized according to the procedure described in **5a**.

*4.1.2.10 N-(6-bromoquinazolin-4-yl)-N,N-dimethylpropane-1,3-diamine (**5b**)*

93.8% yield. mp 95-97 ºC. ^{1}H NMR (600 MHz, DMSO) δ 8.54 (d, *J* = 2.2 Hz, 1H, Ar-H), 8.49 (s, 1H, Ar-H), 8.46 (t, *J* = 5.4 Hz, 1H, NH), 7.88 (dd, *J* = 8.8, 2.2 Hz, 1H, Ar-H), 7.62 (d, *J* = 8.8 Hz, 1H, Ar-H), 3.54 (dd, *J* = 12.6, 7.0 Hz, 2H, CH_2), 2.41 (t, *J* = 7.1 Hz, 2H, CH_2), 2.23 (s, 6H, CH_3), 1.85 -1.76 (m, 2H, CH_2). ESI-MS: m/z 309.2 $[M+H]^+$.

*4.1.2.11 6-bromo-N-(2-morpholinoethyl)quinazolin-4-amine (**5c**)*

94.3% yield. mp 118-120 ºC. ^{1}H NMR (600 MHz, DMSO) δ 8.53 (d, *J* = 2.1 Hz, 1H, Ar-H), 8.48 (s, 1H, Ar-H), 8.39 (t, *J* = 5.1 Hz, 1H, NH), 7.88 (dd, *J* = 8.8, 2.1 Hz, 1H, Ar-H), 7.62 (d, *J* = 8.8 Hz, 1H, Ar-H), 3.56 (m, 6H, CH_2), 2.38 (d, *J* = 6.8 Hz, 4H, CH_2), 1.86 - 1.76 (m, 2H, CH_2). ESI-MS: m/z 337.2 $[M+H]^+$.

*4.1.2.12 6-bromo-N-(3-morpholinopropyl)quinazolin-4-amine (**5d**)*

91.7% yield. mp 127-129 ºC. ^{1}H NMR (600 MHz, DMSO) δ 8.55 (d, *J* = 2.0 Hz, 1H, Ar-H), 8.49 (s, 1H, Ar-H), 8.38 (t, *J* = 4.7 Hz, 1H, NH), 7.89 (dd, *J* = 8.8, 2.1 Hz, 1H, Ar-H), 7.62 (d, *J* = 8.8 Hz, 1H, Ar-H), 3.67 (dd, *J* = 12.5, 6.5 Hz, 2H, CH_2), 3.62 - 3.54 (m, 4H, CH_2), 2.60 (s, 2H, CH_2),

ACCEPTED MANUSCRIPT

2.47 (s, 4H, CH_2), 1.92 (s, 2H, CH_2). ESI-MS: m/z 351.1 $[M+H]^+$.

*4.1.2.13 6-bromo-N-(pyridin-4-ylmethyl)quinazolin-4-amine (**5e**)*

89.1% yield. mp 175-177 ºC. ^{1}H NMR (600 MHz, DMSO) δ 9.03 (t, *J* = 5.6 Hz, 1H, NH), 8.53 (d, *J* = 1.9 Hz, 1H, Ar-H), 8.50 (d, *J* = 4.8 Hz, 2H, Ar-H), 8.42 (s, 1H, Ar-H), 7.89 (dd, *J* = 8.9, 2.0 Hz, 1H, Ar-H), 7.62 (d, *J* = 8.9 Hz, 1H, Ar-H), 7.35 (d, *J* = 5.3 Hz, 2H, Ar-H), 4.80 (d, *J* = 5.7 Hz, 2H, CH_2). ESI-MS: m/z 315.1 $[M+H]^+$.

4.1.2.14

*N-(5-(4-((2-(dimethylamino)ethyl)amino)quinazolin-6-yl)-2-methoxypyridin-3-yl)methanesulfonamide (**6a**)*

·. DMF was removed under reduced pressure and the residue was purified through a column chromatography on silica with chloroform/methanol (V:V 20:1) as a white solid (0.15 g, 58.3% yield). mp 256-258 ºC. ^{1}H NMR (600 MHz, DMSO) δ 9.26 (s, 1H, NH), 8.92 (s, 1H, Ar-H), 8.61 (s, 1H, Ar-H), 8.51 (s, 1H, Ar-H), 8.26 (s, 1H, NH), 8.08 (s, 2H, Ar-H), 7.79 (s, 1H, Ar-H), 3.99 (s, 3H, OCH_3), 3.92 (brs, 2H, CH_2), 3.31 (brs, 2H, CH_2), 3.17 (s, 3H, CH_3), 2.76 (s, 6H, CH_3). ^{13}C NMR (150 MHz, DMSO) δ 164.0, 159.4, 156.5, 154.9, 148.3, 141.2, 133.7, 131.2, 130.9, 128.7, 128.0, 121.2, 120.7, 115.3, 55.6, 53.7, 42.6, 41.0, 36.0. HRMS: m/z 417.1716 $[M+H]^+$.

Compounds **6b-l** was synthesized according to the procedure described in **6a**.

4.1.2.15

*N-(5-(4-((2-(dimethylamino)ethyl)amino)quinazolin-6-yl)-2-methoxypyridin-3-yl)butane-1-sulfonamide (**6b**)*

67.4% yield. mp 108-110 ºC.^{1}H NMR (600 MHz, DMSO) δ 8.57 (d, *J* = 1.5 Hz, 1H, Ar-H), 8.50 (d, *J* = 2.3 Hz, 2H, Ar-H), 8.48 (s, 1H, NH), 8.07 (dd, *J* = 8.7, 1.8 Hz, 1H, Ar-H), 8.05 (d, *J* =

ACCEPTED MANUSCRIPT

2.3 Hz, 1H, Ar-H), 7.77 (d, *J* = 8.6 Hz, 1H, Ar-H), 3.99 (s, 3H, OCH_3), 3.78 - 3.70 (m, 2H, CH_2), 3.18 - 3.10 (m, 2H, CH_2), 2.73 (brs, 2H, CH_2), 2.36 (brs, 6H, CH_3), 1.74 (dt, *J* = 15.3, 7.7 Hz, 2H, CH_2), 1.40 (dq, *J* = 14.7, 7.4 Hz, 2H, CH_2), 0.89 (t, *J* = 7.4 Hz, 3H, CH_3). ^{13}C NMR (150 MHz, DMSO) δ162.2, 159.4, 156.6, 155.1, 148.4, 141.3, 133.6, 132.2, 130.8, 128.9, 128.2, 121.1, 120.0, 115.2, 57.2, 53.7, 52.0, 44.7, 25.1, 20.7, 13.4. HRMS: m/z 459.2147 $[M+H]^+$.

4.1.2.16

*N-(5-(4-((2-(dimethylamino)ethyl)amino)quinazolin-6-yl)-2-methoxypyridin-3-yl)-4-fluorobenzenesulfonamide (**6c**)*

56.9% yield. mp 215-218 ºC. ^{1}H NMR (600 MHz, DMSO) δ 10.05 (s, 1H, NH), 8.53 (d, *J* = 1.6 Hz, 1H, Ar-H), 8.48 (s, 1H, Ar-H), 8.43 (t, *J* = 5.2 Hz, 1H, NH), 8.40 (d, *J* = 2.3 Hz, 1H, Ar-H), 8.04 (d, *J* = 2.4 Hz, 1H, Ar-H), 8.02 (dd, *J* = 8.6, 1.8 Hz, 1H, Ar-H), 7.83 - 7.78 (m, 2H, Ar-H), 7.76 (d, *J* = 8.6 Hz, 1H, Ar-H), 7.40 (t, *J* = 8.8 Hz, 2H, Ar-H), 3.71 (dd, *J* = 12.2, 6.4 Hz, 2H, CH_2), 3.64 (s, 3H, OCH_3), 2.66 (t, *J* = 6.7 Hz, 2H, CH_2), 2.31 (s, 6H, CH_3). ^{13}C NMR (150 MHz, DMSO) δ 164.1 (d, *J* = 249.3 Hz), 159.4, 156.9, 155.1, 148.4, 141.4, 137.2, 133.6, 132.2, 130.6, 129.58 (d, *J* = 9.5 Hz), 128.7, 128.2, 121.4, 120.0, 115.9 (d, *J* = 22.5 Hz), 115.2, 57.4, 53.2, 45.0, 38.2. HRMS: m/z 497.1738 $[M+H]^+$.

4.1.2.17

*N-(5-(4-((2-(dimethylamino)ethyl)amino)quinazolin-6-yl)-2-methoxypyridin-3-yl)-2,4-difluorobenzenesulfonamide (**6d**)*

64.3% yield. mp 197-199 ºC. ^{1}H NMR (600 MHz, DMSO) δ 8.57 - 8.43 (m, 3H, Ar-H and NH), 8.35 (d, *J* = 1.7 Hz, 1H, Ar-H), 7.99 (t, *J* = 16.3 Hz, 2H, Ar-H), 7.77 (dd, *J* = 15.1, 8.4 Hz, 2H, Ar-H), 7.51 (dd, *J* = 13.8, 5.2 Hz, 1H, Ar-H), 7.18 (dd, *J* = 11.7, 4.9 Hz, 1H, Ar-H), 3.76 (d, *J* = 5.0 Hz, 2H,

ACCEPTED MANUSCRIPT

CH_2), 3.66 (s, 3H, CH_3), 2.81 (t, *J* = 6.1 Hz, 2H, CH_2), 2.42 (s, 6H, CH_3). ^{13}C NMR (150 MHz, DMSO) δ 164.5 (dd, *J* = 11.4, 251.1 Hz), 162.2, 159.4, 159.3 (dd, *J* = 13.2, 255.2 Hz), 157.6, 155.0, 148.3, 140.4, 133.8, 132.5, 131.6 (d, *J* = 10.4 Hz), 130.6, 128.7, 128.2, 126.4 (dd, *J* = 3.6, 14.9 Hz), 122.5, 119.8, 115.2, 111.3 (dd, *J* = 2.7, 21.5 Hz), 105.5 (t, *J* = 26.0 Hz), 57.1, 53.1, 44.5, 37.8. HRMS: m/z 515.1632 $[M+H]^+$.

4.1.2.18

*N-(5-(4-((3-(dimethylamino)propyl)amino)quinazolin-6-yl)-2-methoxypyridin-3-yl)butane-1-sulfonamide (**6e**)*

58.6% yield. mp 45-47 ºC. ^{1}H NMR (600 MHz, DMSO) δ 8.66 (brs, 1H, NH), 8.59 (s, 1H, Ar-H), 8.51 (d, *J* = 2.1 Hz, 1H, Ar-H), 8.49 (s, 1H, Ar-H), 8.08 (dd, *J* = 8.6, 1.3 Hz, 1H, Ar-H), 8.06 (d, *J* = 2.1 Hz, 1H, Ar-H), 7.77 (d, *J* = 8.6 Hz, 1H, Ar-H), 3.99 (s, 3H, OCH_3), 3.63 (dd, *J* = 11.8, 6.2 Hz, 2H, CH_2), 3.19 - 3.11 (m, 2H, CH_2), 2.92 - 2.88 (m, 2H, CH_2), 2.58 (s, 6H, CH_3), 2.02 - 1.94 (m, 2H, CH_2), 1.74 (dt, *J* = 15.3, 7.7 Hz, 2H, CH_2), 1.46 - 1.34 (m, 2H, CH_2), 0.89 (t, *J* = 7.4 Hz, 3H, CH_3). ^{13}C NMR (150 MHz, DMSO) δ 162.2, 159.4, 156.6, 155.1, 148.4, 141.3, 132.1, 130.8, 128.9, 128.2, 121.1, 120.1, 115.2, 55.3, 53.7, 52.0, 43.1, 37.9, 25.1, 21.0, 20.7, 13.5. HRMS: m/z 473.2307 $[M+H]^+$.

4.1.2.19

*N-(5-(4-((3-(dimethylamino)propyl)amino)quinazolin-6-yl)-2-methoxypyridin-3-yl)-2,4-difluorobenzenesulfonamide (**6f**)*

56.9% yield. mp 48-50 ºC. ^{1}H NMR (600 MHz, DMSO) δ 8.61 (s, 1H, NH), 8.54 (d, *J* = 1.8 Hz, 1H, Ar-H), 8.48 (d, *J* = 4.6 Hz, 1H, Ar-H), 8.38 (d, *J* = 2.3 Hz, 1H, Ar-H), 8.02 (dd, *J* = 8.0, 2.1 Hz, 2H, Ar-H), 7.80 - 7.73 (m, 2H, Ar-H), 7.55 - 7.49 (m, 1H, Ar-H), 7.18 (td, *J* = 8.5, 2.4 Hz, 1H, Ar-H),

ACCEPTED MANUSCRIPT

3.66 (s, 3H, OCH_3), 3.63 (dd, *J* = 12.0, 6.6 Hz, 2H, CH_2), 2.92 - 2.85 (m, 2H, CH_2), 2.57 (s, 6H, CH_3), 2.02 - 1.95 (m, 2H, CH_2). ^{13}C NMR (150 MHz, DMSO) δ 164.5 (dd, *J* = 11.7, 251.4 Hz), 159.4, 159.3 (dd, *J* = 13.2, 255.3 Hz), 157.6, 155.0, 148.3, 140.7, 133.8, 132.8 (d, *J* = 1.7 Hz), 131.6 (d, *J* = 10.8 Hz), 130.6, 128.7, 128.2, 126.2 (dd, *J* = 1.7, 14.0 Hz), 122.2, 120.0, 111.4 (dd, *J* = 3.2, 21.8 Hz), 105.5 (t, *J* = 26.0 Hz), 55.3, 53.1, 43.1, 38.0, 24.7. HRMS: m/z 529.1734 $[M+H]^+$.

4.1.2.20

N-(2-methoxy-5-(4-((2-morpholinoethyl)amino)quinazolin-6-yl)pyridin-3-yl)butane-1-sulfonamide ***(6g)***

58.1% yield. mp 113-116 ºC. ^{1}H NMR (600 MHz, DMSO) δ 9.46 (s, 1H, NH), 8.54 (d, *J* = 1.2 Hz, 1H, Ar-H), 8.49 (d, *J* = 2.2 Hz, 1H, Ar-H), 8.48 (s, 1H, Ar-H), 8.44 (t, *J* = 5.1 Hz, 1H, NH), 8.07 (dd, *J* = 9.4, 1.8 Hz, 2H, Ar-H), 7.77 (d, *J* = 8.6 Hz, 1H, Ar-H), 4.00 (s, 3H, OCH_3), 3.72 (dd, *J* = 12.4, 6.4 Hz, 2H, CH_2), 3.66 - 3.52 (m, 4H, CH_2), 3.19 - 3.09 (m, 2H, CH_2), 2.64 (t, *J* = 6.8 Hz, 2H, CH_2), 2.50 (d, *J* = 9.7 Hz, 4H, CH_2), 1.75 (dt, *J* = 15.3, 7.7 Hz, 2H, CH_2), 1.46 - 1.35 (m, 2H, CH_2), 0.89 (t, *J* = 7.4 Hz, 3H, CH_3). ^{13}C NMR (150 MHz, DMSO) δ 159.4, 156.6, 155.2, 148.4, 141.3, 133.6, 132.2, 130.7, 128.9, 128.2, 121.1, 119.9, 115.1, 66.0, 56.8, 53.7, 53.3, 52.0, 39.7, 25.1, 20.7, 13.4. HRMS: m/z 501.2233 $[M+H]^+$.

4.1.2.21

*2,4-difluoro-N-(2-methoxy-5-(4-((2-morpholinoethyl)amino)quinazolin-6-yl)pyridin-3-yl)benzenesulfonamide (**6h**)*

59.4% yield. mp 234-236 ºC. ^{1}H NMR (600 MHz, DMSO) δ 10.40 (s, 1H, NH), 8.55 (d, *J* = 1.6 Hz, 1H, Ar-H), 8.49 (d, *J* = 2.4 Hz, 2H, Ar-H), 8.44 (t, *J* = 5.2 Hz, 1H, NH), 8.21 - 8.02 (m, 2H, Ar-H), 7.75 (dd, *J* = 13.0, 8.6 Hz, 2H, Ar-H), 7.68 - 7.54 (m, 1H, Ar-H), 7.21 (td, *J* = 8.5, 2.2 Hz, 1H,

ACCEPTED MANUSCRIPT

Ar-H), 3.73 (dd, J = 12.5, 6.5 Hz, 2H, CH_2), 3.64 (s, 3H, OCH_3), 3.60 (t, J = 4.4 Hz, 4H, CH_2), 2.64 (t, J = 6.9 Hz, 2H, CH_2), 2.52 - 2.51 (m, 4H, CH_2). ^{13}C NMR (150 MHz, DMSO) δ 164.9 (dd, J = 11.6, 252.3 Hz), 159.4, 159.3 (dd, J = 13.4, 256.1 Hz), 157.8, 155.2, 148.4, 142.5, 134.7, 133.3, 131.7 (d, J = 10.7 Hz), 130.5, 128.8, 128.2, 125.2 (dd, J = 3.5, 14.6 Hz), 120.0, 119.8, 115.2, 111.6 (dd, J = 3.2, 22.1 Hz), 105.6 (t, J = 26.0 Hz), 66.0, 56.9, 53.3, 48.5, 37.7. HRMS: m/z 557.1753 $[M+H]^+$.

4.1.2.22

*N-(2-methoxy-5-(4-((3-morpholinopropyl)amino)quinazolin-6-yl)pyridin-3-yl)butane-1-sulfonamide (**6i**)*

67.5% yield. mp 140-142 ºC. ^{1}H NMR (600 MHz, DMSO) δ 9.47 (s, 1H, NH), 8.56 (s, 1H, Ar-H), 8.49 (d, J = 2.2 Hz, 1H, Ar-H), 8.47 (d, J = 4.4 Hz, 1H, Ar-H), 8.07 (d, J = 1.7 Hz, 1H, Ar-H), 8.05 (d, J = 1.9 Hz, 1H, Ar-H), 7.76 (d, J = 8.6 Hz, 1H, Ar-H), 3.99 (s, 3H, OCH_3), 3.67 - 3.55 (m, 6H, CH_2), 3.16 - 3.09 (m, 2H, CH_2), 2.41 (d, J = 7.3 Hz, 6H, CH_2), 1.85 (dt, J = 14.3, 7.1 Hz, 2H, CH_2), 1.79 - 1.69 (m, 2H, CH_2), 1.40 (dq, J = 14.8, 7.4 Hz, 2H, CH_2), 0.89 (t, J = 7.4 Hz, 3H, CH_3). ^{13}C NMR (150 MHz, DMSO) δ 159.3, 156.6, 155.2, 148.4, 141.3, 133.6, 132.2, 130.7, 128.9, 128.2, 121.2, 120.0, 115.2, 66.0, 55.9, 53.7, 53.2, 52.0, 25.3, 25.1, 21.0, 20.7, 13.4. HRMS: m/z 515.2407 $[M+H]^+$.

4.1.2.23

*2,4-difluoro-N-(2-methoxy-5-(4-((3-morpholinopropyl)amino)quinazolin-6-yl)pyridin-3-yl)benzenesulfonamide (**6j**)*

61.9% yield. mp 178-180 ºC. ^{1}H NMR (600 MHz, DMSO) δ 10.55 (s, 1H, NH), 8.56 (d, J = 1.5 Hz, 1H, Ar-H), 8.50 - 8.47 (m, 2H, Ar-H and NH), 8.46 (d, J = 2.2 Hz, 1H, Ar-H), 8.07 (d, J = 2.2

ACCEPTED MANUSCRIPT

Hz, 1H, Ar-H), 8.04 (dd, *J* = 8.6, 1.7 Hz, 1H, Ar-H), 7.80 - 7.71 (m, 2H, Ar-H), 7.59 - 7.52 (m, 1H, Ar-H), 7.19 (td, *J* = 8.5, 2.2 Hz, 1H, Ar-H), 3.64 (s, 3H, OCH_3), 3.62 - 3.56 (m, 6H, CH_2), 2.43 (m, 6H, CH_2), 1.90 - 1.82 (m, 2H, CH_2). ^{13}C NMR (150 MHz, DMSO) δ164.8 (dd, *J* = 11.3, 252.0 Hz), 159.3, 159.2 (dd, *J* = 13.5, 255.9 Hz), 157.7, 155.2, 148.4, 141.9, 134.1, 133.3, 131.7 (d, *J* = 10.8 Hz), 130.5, 128.8, 128.2, 125.5 (dd, *J* = 1.4, 13.7 Hz), 120.6, 119.9, 111.5 (dd, *J* = 3.2, 22.1 Hz), 105.6 (t, *J* = 26.0 Hz), 66.0, 55.8, 53.2, 53.1, 38.8, 25.2. HRMS: m/z 571.1905 $[M+H]^+$.

4.1.2.24

*N-(2-methoxy-5-(4-((pyridin-4-ylmethyl)amino)quinazolin-6-yl)pyridin-3-yl)butane-1-sulfonamide (**6k**)*

66.7% yield. mp 57-59 ºC. ^1H NMR (600 MHz, DMSO) δ 9.47 (s, 1H, NH), 9.09 (t, *J* = 5.7 Hz, 1H), 8.66 (s, 1H, Ar-H), 8.51 (d, *J* = 6.4 Hz, 3H, Ar-H), 8.46 (s, 1H, NH), 8.13 (d, *J* = 8.7 Hz, 1H, Ar-H), 8.09 (d, *J* = 1.8 Hz, 1H, Ar-H), 7.81 (d, *J* = 8.6 Hz, 1H, Ar-H), 7.38 (d, *J* = 5.2 Hz, 2H, Ar-H), 4.85 (d, *J* = 5.6 Hz, 2H, CH_2), 3.99 (s, 3H, CH_3), 3.14 (t, *J* = 7.8 Hz, 2H, CH_2), 1.77 - 1.72 (m, 2H, CH_2), 1.43 - 1.37 (m, 2H, CH_2), 0.89 (t, *J* = 7.4 Hz, 3H, CH_3). ^{13}C NMR (150 MHz, DMSO) δ 159.4, 156.7, 155.0, 149.5, 148.4, 148.3, 141.4, 133.9, 132.3, 131.0, 128.8, 128.3, 122.1, 121.1, 120.0, 115.0, 53.7, 52.0, 42.6, 25.1, 20.7, 13.4. HRMS: m/z 479.1847 $[M+H]^+$.

4.1.2.25

*2,4-difluoro-N-(2-methoxy-5-(4-((pyridin-4-ylmethyl)amino)quinazolin-6-yl)pyridin-3-yl)benzenesulfonamide (**6l**)*

62.4% yield. mp 121-123 ºC. ^1H NMR (600 MHz, DMSO) δ 10.41 (s, 1H, NH), 9.10 (t, *J* = 5.8 Hz, 1H, NH), 8.68 (d, *J* = 1.7 Hz, 1H, Ar-H), 8.54 (d, *J* = 2.3 Hz, 1H, Ar-H), 8.52 (d, *J* = 5.5 Hz, 2H, Ar-H), 8.47 (s, 1H, Ar-H), 8.14 (dd, *J* = 10.6, 2.1 Hz, 2H, Ar-H), 7.81 (d, *J* = 8.7 Hz, 1H, Ar-H), 7.76

ACCEPTED MANUSCRIPT

(td, J = 8.5, 6.6 Hz, 1H, Ar-H), 7.64 - 7.56 (m, 1H, Ar-H), 7.39 (d, J = 5.8 Hz, 2H, Ar-H), 7.21 (td, J = 8.5, 2.3 Hz, 1H, Ar-H), 4.87 (d, J = 5.6 Hz, 2H, CH_2), 3.64 (s, 3H, OCH_3). ^{13}C NMR (150 MHz, DMSO) δ 164.96 (dd, J = 11.7, 253.9Hz), 159.5, 159.4 (dd, J = 13.4, 256.1Hz), 157.9, 155.0, 149.5, 148.4 (d, J = 18.7 Hz), 142.8, 135.1, 133.1, 131.7 (d, J = 10.8 Hz), 130.8, 128.7, 128.3, 125.1 (dd, J = 3.5, 14. 5 Hz), 122.1, 120.0, 119.5, 115.1, 111.6 (dd, J = 3.1, 22.1 Hz), 105.7 (t, J = 25.8 Hz), 53.27, 42.65. HRMS: m/z 535.1348 $[M+H]^+$.

4.2 Biological (pharmacological) evaluation

4.2.1 Cell culture

HCT-116, A549, SK-HEP-1, SNU638, MDA-MB-231, MCF7, HEK293 and MRC-5 were purchased from the American Type Culture Collection (Manassas, VA, USA). Cells were grown in DMEM (SNU-638, MCF7, HEK293, MRC-5 and SK-HEP-1) or RPMI1640 (HCT-116, A549 and MDA-MB-231 cells) supplemented with 10% FBS and antibiotics-antimycotics (PSF; 100 units/mL penicillin G sodium, 100 μg/mL streptomycin, and 250 ng/mL amphotericin B) in a humidified incubator containing 5% CO_2 at 37 °C.

4.2.2 Antiproliferative activity

The cell viability was evaluated using the sulforhodamine B (SRB) cellular protein-staining method with minor modifications. Briefly, cells were treated with various concentrations of compounds in 96-well plates and incubated at 37 °C in a humidified atmosphere with 5% CO_2 for 72 h. After treatment, the cells were fixed with 10% TCA solution, and cell viability was determined with the SRB assay. The percentage of cell-growth inhibition was calculated using the formulae below. The IC_{50} values were calculated using a non-linear regression analysis (percent growth versus concentration).

ACCEPTED MANUSCRIPT

% growth inhibition = 100 - 100×(OD_{sample} - OD_{Day0}) / ($OD_{Neg\ control}$ - OD_{Day0})

4.2.3 PI3K enzymatic activity assay

The PI3K kinase assay was measured by PI3 Kinase Activity/Inhibitor Assay Kit (EMD Millipore) following the manufacturer's protocols.

4.2.4 Molecular docking studies

The crystal structure of PI3Kα (PDB entry code: 4ZOP/ 5ITD) in complex with 4Q2 was used for molecular modeling. The AutoDock 4.2 was used to perform docking calculations. Polar hydrogens and partial charges were added for PI3Kα protein using the Kollman United Atom charges with Sybyl 6.9.1, and energy minimization was made employing both steepest descent and conjugate gradients protocols. Atomic solvation parameters and fragmental volumes for the proteins were assigned using the addsol utility in the AutoDock 4.2 program. A 60 × 60 × 60 Å grid box with a grid spacing of 0.375 Å was generated for the receptor. Affinity grid fields were generated using the auxiliary program AutoGrid 4.0. The Lamarckian genetic algorithm (LGA) was used to find the appropriate binding positions, orientations, and conformations of the ligands. The optimized AutoDocking parameters are as follows: the maximum number of energy evaluations was increased to 25,000,000 per run; the iterations of Solis & Wets local search was 3000; the number of individuals in population was 300 and the number of generations was 100. Results differing by less than 2 Å in a positional root mean square deviation (RMSD) were clustered together. In each group, the lowest binding energy configuration with the highest % frequency was selected as the group representative. All other parameters were maintained as default. Accelrys Discovery Studio Visualizer 4.0 was used for graphic display.

4.2.5 Cell cycle analysis

ACCEPTED MANUSCRIPT

Cells cycle analysis was carried out as described previously [39]. Cells were plated in 100mm-diameter culture dishes and cultured overnight. Then cells were treated with indicated concentration of **6b** for 24 h. The floating and adherent cells were collected and fixed in cold 70% ethanol at -20 °C overnight. After washing with PBS for 3 times, cells were treated with 100 μg/mL RNase A at room temperature for 30 min and then stained with 50 μg/mL propidium iodide (PI) for another 30 min in the dark before subjected to flow cytometric analysis.

4.2.6 Annexin V assay

Cell apoptosis was evaluated using Annexin V FITC/PI apoptosis detection kit (BD Biosciences, CA, USA) according to the manufacture's instruction.

4.2.7 Western blot analysis

Cells were treated with various concentration of **6b**. Western blot analysis was carried out as described previously [35]. Blots were imaged by Image Quant LAS 4000 (GE Healthcare Life Sciences, USA). Antibodies for PI3 Kinase p110α, Phospho-PI3 Kinase p85 (Tyr458)/p55 (Tyr199), Phospho-Akt (Ser473), Phospho-GSK-3 alpha/beta (Ser21/9), GSK-3β, Cyclin D1, Cleaved Caspase-3 (Asp175) and Cleaved Caspase-9 were purchased from Cell Signaling Technology (Danvers, MA, USA). Antibodies for CDK2, p27, Bax, Cytochrome *c* and Bcl-2 were purchased from Santa Cruz Biotechnology (Santa Cruz, CA, USA).

4.2.8 Immunofluorescence microscopy

Cells were cultured on a confocal dish coated with 0.2% gelatin. After **6b** treatment (0.5μM) for 8 h, the cells were fixed with 4% paraformaldehyde for 20 min and rinsed with washing buffer 3 times before blocking with 1% BSA. The cells were incubated with the p-Akt (Ser473) antibody at

ACCEPTED MANUSCRIPT

4 °C overnight and then incubated with the second antibody before DAPI staining. The cells were visualized under a fluorescence reverse microscope (Leica TCS SP8, Germany). The images were recorded with a Leica TCS SP8 confocal microscope using a 40x silicone oil objective (40x/1.30 NA).

Conflicts of interest

The authors declare that there are no conflicts of interest.

Acknowledgments

Financial supported by Liaoning Provincial Department of Education (Grant No. L2015514) and Career Development Support Plan for Young and Middle-aged Teachers in Shenyang Pharmaceutical University (Grant No. ZQN2015023).

References

1. Leevers SJ, Vanhaesebroeck B, Waterfield MD. *Curr. Opin. Cell. Biol.*, 1999, 11(2):219-225.
2. Liu P, Cheng H, Roberts T M, et al. *Nat. Rev. Drug. Disco.*, 2009, 8(8):627-644.
3. Engelman JA. *Nat. Rev. Cancer.* 2009, 9(8):550-562.
4. Hennessy BT, Smith DL, Ram PT, Lu Y, Mills GB. *Nat. Rev. Drug Discov.* 4(12) (2005) 988-1004.
5. Akinleye A, Avvaru P, Furqan M, Song Y, Liu D. J. *Hematol. Oncol.* 2013, 6(1):88.
6. Chen Y, Zhang L, Yang C, et al. *Bioorg. Med. Chem.* 2016, 24(5):957-966.
7. LM Thorpe, H Yuzugullu, JJ Zhao. *Nat. Rev. Cancer.* 2015, 15(1):7-24.
8. Yap TA, Bjerke L, Clarke PA, et al. *Curr. Opin. Pharmacol.* 2015, 23:98-107.
9. Liang J, Slingerland JM. *Cell Cycle.* 2003, 2(4):339-345.
10. Prasad SB, Yadav SS, Das M, et al. *Cell. Oncol.* 2015, 38(3):215-225.

ACCEPTED MANUSCRIPT

ACCEPTED MANUSCRIPT

11. Zhou S, Liu L, Li H, et al. *Brit J Cancer.* 2014, 110(10):2479-2488.

12. Mayo LD, Dixon JE, Durden DL, et al. *J. Biol. Chem.* 2002, 277(7):5484-5489.

13. Ola MS, Nawaz M, Ahsan H. Mol. *Cell. Biochem.* 2011, 351(1-2):41-58.

14. Lee W S, Yi S M, Yun J W, et al. *J. Cancer Prev.* 2014, 19(1):14-22.

15. Volinia S, Hiles I, Ormondroyd E, et al. *Genomics.* 1994, 24(3):472-477.

16. Lai YL, Mau BL, Cheng WH, et al. *Ann.Surg. Oncol.* 2008, 15(4):1064.

17. Baohua Y, Xiaoyan Z, Tiecheng Z, et al. *Diagn. Mol. Pathol.* 2008, 17(3):159-165.

18. Dirican E, Akkiprik M, Özer A. *Tumor Biol.* 2016, 37(6):7033-7045.

19. Asati V, Mahapatra DK, Bharti SK. *Eur. J. Med. Chem.* 2016, 109:314-341.

20. Britten CD. Cancer. Chemoth. *Pharm.* 2013, 71(6):1395-1409.

21. Welker ME, Kulik G. *Bioorg. Med. Chem.* 2013, 21(14):4063-4091.

22. Britten CD. Mol. *Cancer. Ther.* 2013, 71(6):1395-1409.

23. Chang KY, Tsai SY, Wu CM, et al. *Clin Cancer Res.* 2011, 17(22):7116-7126.

24. Cheng H, Li C, Bailey S, et al. *Acs. Med. Chem. Lett.* 2012, 4(1):91-97.

25. Knight SD, Adams ND, Burgess JL, et al. *Acs. Med. Chem. Lett.* 2010, 1(1):39-43.

26. Kim O, Jeong Y, Lee H, et al. *J. Med. Chem.* 2011, 54(7):2455-2466.

27. Down KD, Amour A, Baldwin IR, et al. *J. Med. Chem.* 2015, 58(18):7381-7399.

28. Xi L, Zhang JQ, Liu ZC, et al. *Org. Biomol. Chem.* 2013, 11(26):4367-4378.

29. Yadav RR, Guru SK, Joshi P, et al. *Eur. J. Med. Chem.* 2016, 122:731-743.

30. Hoegenauer K, Soldermann N, Stauffer F, et al. *Acs. Med. Chem. Lett.* 2016, 7(8):762-767.

31. Xin M, Hei Y Y, Zhang H, et al. *Bioorg. Med. Chem. Lett.* 2017, 27(9):1972-1977.

32. Zhang H, Xin M H, Xie X X, et al. *Bioorg. Med. Chem.* 2015, 23(24):7765-7776.

ACCEPTED MANUSCRIPT

ACCEPTED MANUSCRIPT

33. Frys S, Czuczman NM, Mavis C, et al. *Blood.* 2014, 82(981):764-770.

34. Bhatti M, Ippolito T, Mavis C, et al. *Dtsch. Med. Wochenschr.* 2015, 102(41):1477-1480.

35. Vasudevan K M, Barbie D A, Davies M A, et al. *Cancer Cell.* 2009, 16(1):21-32.

36. Chen JN, Wang XF, Li T, et al. *Eur. J. Med. Chem.* 2016, 107: 12-25.

37. Solomon VR, Lee H. *Curr. Med. Chem.* 2011, 18(10):1488-1508.

38. Lin S W, Wang C Y, Ji M, et al. *Bioorg. Med. Chem.* 2018. https://doi.org/10.1016/j.bmc.2017.12.025.

39. Fan Y H, Li W, Liu D D, et al. *Eur. J. Med. Chem.* 2017, 139:95-106.

ACCEPTED MANUSCRIPT

ACCEPTED MANUSCRIPT

Figures legends

Scheme 1. (a) benzenesulfonyl chloride, pyridine, rt, 24 h; (b) bis(pinacolato)diborane, $Pd(dppf)_2Cl_2$, AcOK, DMF, 100 ºC, 8 h; (c) amines, isopropanol, 50 ºC, 1h; (d) $Pd(dppf)_2Cl_2$, Cs_2CO_3, DMF/ H_2O, 90 ºC, 8 h.

Fig.1. The design strategy based on NVP-BEZ235 and GSK2292767.

Fig.2. The binding model of **6b** bound to PI3Kα. Autodock 4.2 programs were used to perform this molecular docking simulation. (A) 2D binding model of **6b** and PI3Kα.(B-C) 3D binding model of **6b** and PI3Kα.

Fig.3. 6b suppresses PI3K signaling pathway. (A) The effects of **6b** on the expressions of PI3K-associated signaling proteins in HCT116 cells. (B) The effects of **6b** on the expression level of p-Akt (Ser473) in cells as determined by immunofluorescence analysis. Cells were treated with the indicated concentrations of **6b** for 24 h and then the protein expressions were determined by using Western blot. The alternations of related proteins were quantified using Image J program. $*P<0.05$ or $**P<0.01$ was considered statistically significant compared with corresponding control values.

Fig.4. 6b induced G1 cell cycle arrest in HCT116 cells. (A) Cells were treated with the indicated concentrations of **6b** for 24 h. The DNA content of the cells was then analyzed by flow cytometry analysis as described in Materials and Methods. (B) Cells were treated with the indicated concentrations of **6b** for 24 h and then analyzed the protein expressions associated with the G1 phase cell cycle arrest in HCT116 cells. The changes of corresponding proteins

ACCEPTED MANUSCRIPT

were quantified using Image J. Each bar represents mean ± SEM (n = 3), **P*<0.05 or ***P*<0.01 was considered statistically significant compared with corresponding control values.

Fig.5. 6b induced apoptosis in HCT116 cells. Cells were treated with various concentrations of **6b** for 48 h and then analyzed the Annexin V-FITC/PI staining test by flow cytometry analysis. The number in the right quads of each panel means the percentage of Annexin V positive cells.

Fig.6. (A) The effects of **6b** on the induction of apoptosis were also analyzed by Western blot in HCT116. The changes of corresponding proteins were quantified using Image J. Each bars represent mean ± SE (n = 3). **P*<0.05 or ***P*<0.01 was considered statistically significant compared with corresponding control values.

Fig. S1. The binding model of **6b** bound to PI3Kβ, PI3Kγ and PI3Kδ. (A-B) 2D and 3D binding model of **6b** and PI3Kβ. (C-D) 2D and 3D binding model of **6b** and PI3Kγ. (E-F) 2D and 3D binding model of **6b** and PI3Kδ.

ACCEPTED MANUSCRIPT

ACCEPTED MANUSCRIPT

Highlights

- A series of novel 4-aminoquinazoline derivatives were synthesized and characterized.
- Their antiproliferative activities against cancer cell lines were evaluated.
- **6b** exhibited PI3K inhibitory activity with an IC_{50} value of 13.6 nM.
- **6b** exhibited potent antiproliferative effects via PI3K/Akt signaling pathway inhibition.
- Compound **6b** induced G1 phase arrest and apoptosis via the mitochondrial pathway.

ACCEPTED MANUSCRIPT